Received: 14 February 2021 | Revised: 29 March 2021 | Accepted: 1 April 2021

DOI: 10.1002/apj.2646

RESEARCH ARTICLE

Asia-Pacific Journal of Chemical Engineering | Curtin University | WILEY

Graphene oxide-carboxymethyl cellulose hydrogel beads for uptake and release study of doxorubicin

Aning Ayucitra[1,2] | **Artik Elisa Angkawijaya**[3] | **Yi-Hsu Ju**[1,3,4] | **Chintya Gunarto**[1,2] | **Alchris Woo Go**[3] | **Suryadi Ismadji**[2,1]

[1]Department of Chemical Engineering, National Taiwan University of Science and Technology, Taipei, Taiwan

[2]Department of Chemical Engineering, Widya Mandala Surabaya Catholic University, Surabaya, Indonesia

[3]Graduate Institute of Applied Science and Technology, National Taiwan University of Science and Technology, Taipei, Taiwan

[4]Taiwan Building Technology Center, National Taiwan University of Science and Technology, Taipei, Taiwan

Correspondence
Artik Elisa Angkawijaya, Graduate Institute of Applied Science and Technology, National Taiwan University of Science and Technology, Taipei 10607, Taiwan.
Email: artikelisa@mail.ntust.edu.tw

Funding information
National Taiwan University of Science and Technology, Grant/Award Number: 101H451403; Ministry of Science and Technology of Taiwan, Grant/Award Number: MOST 108-2221-E-011-106

Abstract

Graphene oxide (GO)-based hydrogel beads were synthesized by physical crosslinking of GO with carboxymethyl cellulose (CMC) to produce a pH-sensitive drug carrier with selective drug-release properties. Four different GO/CMC composite hydrogel beads (GCB) were prepared with GO oxidized at 30°C and 5q0°C with varying GO loading 1 or 5 mg/ml. Physicochemical properties of the synthesized GO and its composite beads were provided in this work. A mild oxidation temperature of 50°C produce GO-50 with satisfactory oxidation degree as shown by intensity ratio of D and G bands (I_D/I_G) and carbon to oxygen (C/O) ratios of 0.991 and 1.94, respectively. The highest loading capacity of doxorubicin (DOX) was 4.2494 mg/g for GCB synthesized from GO-50 with dispersion concentration of 5 mg/ml (GCB-50.5), corresponding to its abundant oxygen-containing functional groups. The release profile of DOX also confirmed its strong pH-sensitive behavior. The in vitro cytotoxicity tests on 7F2 cells by MTT assay revealed that GCBs have a higher percentage of viability than that of their GO precursors due to the incorporation of CMC into the beads. The prepared hydrogel beads thus can potentially be used as an effective and viable DOX carrier.

KEYWORDS

Carboxymethyl cellulose, Doxorubicin carrier, Graphene oxide, pH-dependent release

1 | INTRODUCTION

Graphene family nanomaterials (GFNs), such as graphene, reduced graphene oxide (RGO), and graphene oxide (GO), have received great attention due to their large surface area, excellent mechanical and optical properties, and outstanding thermal and electrical conductivity.[1–3] Out of these GFNs, GO comes out as one of the most studied materials due to their profound potential as the building block for many functional materials,[4–6] tailor-made functional properties, and their usability in energy-related materials, wastewater treatment, and biomedical fields.[1,4,5,7–17]

DOX is one of the most common model drugs used in studies related to drug delivery systems.[18–22] This drug belongs to the group of antineoplastics and is commonly used in chemotherapy treatment. However, only a small portion of drug may be transported to the nucleus of cancer cells and worked efficiently.[23] Thus, a compatible drug carrier is needed to deliver the drug to its targeted sites. GO is one possible alternative carrier since DOX can be loaded on GO surface through π–π stacking

interaction or through hydrogen bonding interaction between carboxylic groups of GO an amine groups of DOX.[18,20,24] Since GO tends to agglomerate, are poorly dispersed in a physiological environment, and reportedly can be toxic in a concentration- and cell-dependent manner, many GO-biopolymer composites have been synthesized to eliminate these drawbacks.[15,25–27] Biopolymers such as carboxymethyl cellulose (CMC), chitosan, alginate, and gelatin have been proven to improve solubility and bioavailability of GO, while also tailoring other functionalities such as temperature and pH response.[9,18,20,21,28–32]

Amongst biopolymers, CMC is the most promising material which can be composited with GO for use as drug carrier. A study by Rasoulzadeh and Namazi reported the synthesis of pH-sensitive CMC/GO hydrogel beads.[18] The GO used for the synthesis of these hydrogel beads were produced by a simple modified Hummers' method, which employ sodium nitrate as catalyst. The resultant beads had maximum doxorubicin (DOX) loading about 1.8 g/g and showed no obvious toxicity against SW480 cells. Rasoulzadeh and Namazi postulated that GO-CMC polymeric matrix may protect and sustain-release the drug through the digestive tracks.[18] Another study by Rao et al. reported the preparation of CMC-modified GO with the aid of adipic acid dihydrazide (ADH), *N*-hydroxysulfosuc cinimide (NHS), and 1-ethyl-dimethylaminopropyl carbodiimide (EDC). The CMC-modified GO showed pH-sensitive release profiles and had no toxic effects against NIH-3T3 and Hela cells.[20] To date, reported literatures mainly focused on the potential application of GO and GO/CMC without giving detail information on the impact of synthesis procedure on the formation of hydrophilic functional groups and the extent of oxidation on GO surface which essentially may affect the behavior of GO/CMC as drug carrier.

This present work offers a comprehensive information on the role of GO in tailoring the properties of GO/CMC composite hydrogel beads (GCB) as DOX carrier. An energy-saving, catalyst-free and non-toxic approach of modified Hummers' method was employed to produce GO from graphite powder. To date, no similar work was reported in literature. Inclusive characterizations were performed to investigate the effect of oxidation temperatures on GO properties and on the performances of the derived GCB. GCBs were then synthesized, characterized, and evaluated its DOX-carrying capability. In order to avoid unnecessary toxicity, the GO employed in the GCB synthesis were considerably low compared to other studies. In vitro cytotoxicity study of the prepared materials against 7F2 cell lines was also investigated by MTT assay.

2 | MATERIALS AND METHODS

2.1 | Materials

All chemicals in this work were of analytical grade and used without further purification. Graphite powder (<20 μm), potassium permanganate, hydrogen peroxide, sodium CMC (medium viscosity), iron (III) chloride, and DOX hydrochloride (98.0%–102.0%) were purchased from Sigma-Aldrich (St. Louis, Missouri, USA). Sulfuric acid (98%) was purchased from Scharlau (Sentmenat, Spain). For cytotoxicity study, thiazolyl blue tetrazolium bromide or MTT (3-[4,5-dimethyl-2-thiazolyl]-2,5-diphenyl-2H-tetrazolium bromide) was obtained from Sigma-Aldrich (St. Louis, Missouri, USA), while dimethyl sulfoxide (DMSO) was obtained from J.T. Baker (Avantor, USA). 7F2 cell lines (mouse bone marrow tissues, BCRC No. 60453) were obtained from Bioresource Collection and Research Center (Hsinchu, Taiwan).

2.2 | Synthesis of GO

The GO preparation was adapted from a catalyst-free Hummers' method[33] with modification of oxidation temperature at 30°C and 50°C. Briefly, 1 g of graphite powder was added into 50 ml of concentrated H_2SO_4 and was then left for reaction in an ice bath under constant stirring at 400 rpm. After an hour, 4 g of $KMnO_4$ was then slowly added to the mixture and was left under stirring for another 2 h. This mixture was then transferred to 30°C or 50°C oven for 1-h oxidation reaction. To halt the oxidation process, the mixture was re-placed into an ice bath, and 65 ml of hydrogen peroxide solution (7%) was then added dropwise to the mixture. Afterwards, the resultant yellowish-brown color mixture was then centrifuged 2000 *g* for 30 min and repeatedly washed with deionized (DI) water until neutral pH to obtain yellowish-brown color solid. These solids were then lyophilized at −40°C and $1.3{\cdot}10^{-4}$ atm for 24 h (FreeZone 2.5 Benchtop model 7670520, Labconco, Kansas, USA) and labeled as GO-T where T refers to the oxidation temperature.

2.3 | Synthesis of GCB

GCBs were synthesized following the method described by Rasoulzadeh and Namazi[18] with some modifications. Prior to the synthesis of GCB, GO dispersion at concentration of 1 and 5 mg/ml was prepared by 30-min ultrasonication of lyophilized GO in DI water (TransSonic, New Zealand). To the GO dispersion, 2.5 wt

% of sodium CMC powder was then added and stirred until dissolved fully. This mixture was added dropwise into 0.2-M $FeCl_3$ solution for crosslinking reaction. After 20 min, the formed beads were filtered and washed with DI water. These beads were then lyophilized overnight and labeled as GCB-T-DC where T refers to the oxidation temperature and DC refers to the dispersion concentration of the GO. CMC hydrogel beads were prepared and were used as control; and instead of GO dispersion, DI water is used to solubilize 2.5 wt% of sodium CMC powder.

2.4 | Characterization of the GO and GCB

X-ray powder diffraction (XRD) patterns of graphite, GOs, and GCB were obtained on a Bruker D2 Phaser (Bruker AXS GmbH, Germany) with Cu–Kα radiation (λ = 1.5406 Å) and recorded over a 2θ region of 5–70° with a scanning speed of 5°/min. The interlayer spacing of graphite and GOs was calculated from their diffraction peaks at 2θ with the aid of Bragg's equation. Fourier-transform infrared (FT-IR) spectra of all samples were recorded in the scan range 4000–400 cm^{-1} using a Bio-Rad FTS-3500 (Bio-Rad Laboratories Inc., USA) by the KBr method. Raman spectra of graphite precursor and the prepared GOs were obtained using a UniG2D Raman spectroscope (UniNano Tech Co., Korea), operating at 532-nm excitation wavelength. Surface morphology of the prepared samples was observed on a field emission scanning electron microscope (FESEM JEOL JSM-6500 F, JEOL USA Inc., USA) equipped with an energy dispersive X-ray spectroscopy (EDX) at an acceleration voltage of 15.0 kV. The atomic percentage of the C and O elements (Table S1) were used for the quantification of C/O ratios of GOs. Prior to analysis, all dried samples were sputter coated by platinum for 60 s in a JFC-1200 auto fine coater (JEOL, Tokyo, Japan). Thermal stability of the prepared materials was investigated using a Diamond TG/DTA (Perkin Elmer, USA) in a highly purified nitrogen atmosphere. For all measurements, a platinum crucible pan was used, and temperature program ranged from 30°C to 600°C with a heating rate of 10°C/min.

2.5 | Swelling behavior

To study the swelling behavior of the hydrogel beads, 25-mg beads were allowed immersed in 5 ml of pH-adjusted phosphate buffer saline (PBS) solutions (pH 7.4, 6.8, and 2.1) at 30°C. At predetermined time intervals, samples were taken out and blotted onto filter paper to remove surface water. The swelling capacity of beads was determined according to Equation 1.

$$\text{Swelling}\,(\%) = \frac{(W_2 - W_1)}{W_1} \times 100, \tag{1}$$

where W_1 is the initial weight of dried samples and W_2 is the weight of samples after being immersed in medium for predetermined time.[18]

2.6 | Drug loading and release studies

DOX was used as the model drug to investigate the potential capability of the prepared materials as anticancer drug carrier. Prior to the release study, DOX was loaded onto the prepared nanocomposite materials. To investigate the pH-sensitive functionalities of the prepared materials, drug release study was conducted in acidic cancerous pH (5.0) and physiological pH (7.4).

For the drug loading experimentation, 25 mg of the prepared materials were added to 5 ml of DOX solution (with a concentration of 25 ppm in DI water) under continuous shaking in an incubator at 30°C, 200 rpm, for 72 h in dark condition. The quantity of the drug loaded in the materials was measured by quantifying the amount of unbound DOX using UV–Vis spectroscopy (Jasco, USA) at 480 nm and calculated by using Equation 2 for drug loading capacity (DLC).[18,19] Excess DOX was washed using DI water prior to the release study.

$$\text{Drug loading capacity}\left(\frac{\text{mg}}{\text{g}}\right) = \frac{\textit{amount of drug in material in mg}}{\textit{amount of dry material in g}}. \tag{2}$$

The drug release study was carried out as follows: 25 mg of drug loaded-material were transferred into vials containing 5 ml of PBS solution (pH 7.4 and 5.0) and placed in a continuous shaking incubator at 37°C for 24 h with a shaking speed of 200 rpm. In order to measure the amount of released drug at appropriate time intervals, adequate amount (200 μL) of sample solution was withdrawn and the same volume of fresh buffer solution was then added to maintain the volume of buffer constant. The amount of released drug from nanocomposite materials was quantified from its absorbance using UV–Vis spectroscopy (BioTek® Instruments, USA) at 480 nm. The amount of drug released from materials was calculated by the following formula (Equation 3) as reported by Javanbakht and Namazi.[19]

$$\text{Cumulative drug release}\,(\%) = \frac{\textit{the amount of released drug}}{\textit{the amount of loaded drug}} \times 100 \quad (3)$$

2.7 | In vitro cytotoxicity study

The toxicity of materials towards 7F2 cell lines was investigated in vitro by MTT assay. The cells were firstly cultured in hemoflagellate minimum essential medium (HO-MEM) supplemented with 10% heat-inactivated fetal bovine serum (FBS) and grown to about 80% confluency prior to initiating the assays. Due to the nature of materials being tested, an extract test procedure of ISO 10993-5 described by Wang et al.[34] was followed with some modifications throughout the study. All materials (5 mg/ml) were incubated in culture medium supplemented with serum for 24 h at 37°C after overnight sterilization under UV light irradiation. The extract-containing medium, called as preconditioned medium, was then used to replace the culture media used on cells seeded in a well-plate. The relative cell viability was measured by comparing the absorbance of the sample wells to that of control wells containing only the cells.

3 | RESULTS AND DISCUSSION

GO preparation in this work was done by oxidation of graphite powder at mild temperatures (30°C and 50°C), in the absence of catalyst. These selected temperatures were considerably lower than that of previously developed Hummers' methods (80–98°C).[14,18,19] These synthesized GOs were then characterized by XRD, FT-IR, Raman, and TGA instruments to investigate the effect of oxidation temperatures on the resultant GO's properties. Characterization of the graphite powder as the precursor was also included for comparison.

Figure 1a shows XRD patterns of graphite and GOs prepared at 30°C and 50°C (GO-30 and GO-50, respectively). In Figure 1a (black line), the typical diffraction peak of graphite can be found at $2\theta = 26.71°$ which correspond to an interlayer spacing of 0.33 nm. Upon oxidation, this characteristic diffraction pattern almost disappeared and only a very weak diffraction peak at $2\theta = 27.48°$ can be observed in GO-30, which may be attributed to the incomplete oxidation of graphite to GO.[35] The oxidation also shown to expand the interlayer spacing of GO-30 and GO-50 to 0.72 nm ($2\theta = 12.24°$) and 0.77 nm ($2\theta = 11.64°$), respectively. This happened due to the addition of more oxygen functional groups on GO lattice with an increasing oxidation temperature.

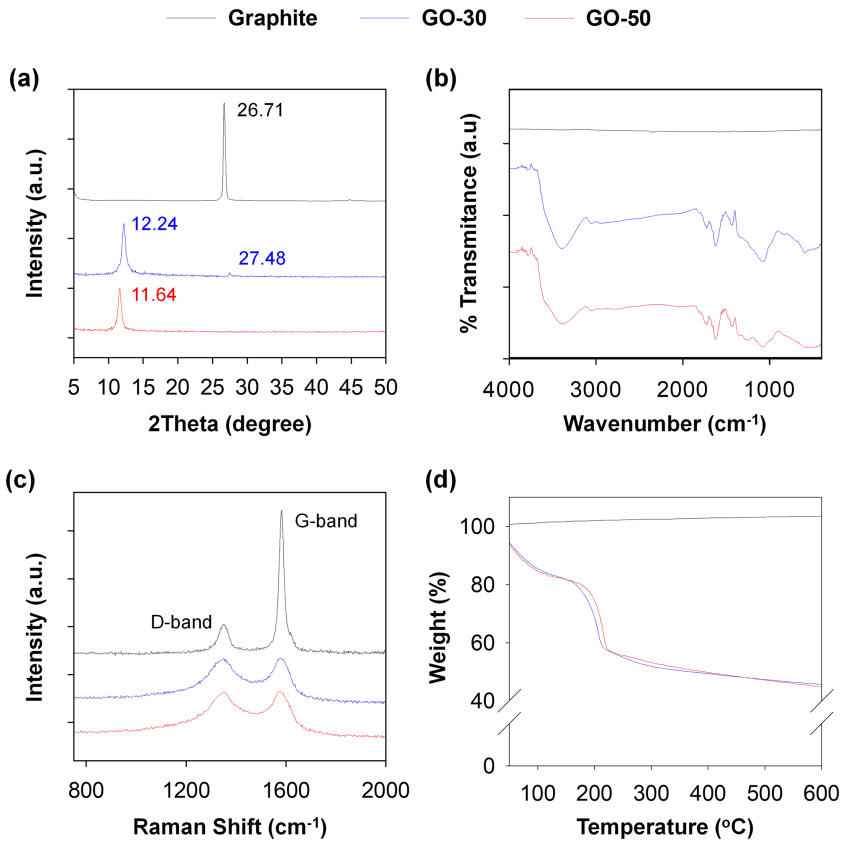

FIGURE 1 (a) XRD patterns, (b) FT-IR spectrum, (c) Raman spectrum, and (d) TGA thermogram of graphite (black lines) and GO synthesized at 30°C (blue lines) or 50°C (red lines)

Since interlayer spacing of the resultant materials is proportional to the degree of oxidation,[36] these XRD results imply that GO-50 may possess higher degree of oxidation compared to GO-30.

To confirm the formation of oxygen functional groups upon oxidation process, the FT-IR spectra of graphite and the GOs were obtained. As shown in Figure 1b, no oxygen-functional groups can be found in the FT-IR spectra of graphite. On the other hand, an intense and broad peak of O–H bond (hydroxyl group) at 3400 cm^{-1} can be observed in both GO-30 and GO-50. In addition, spectra that attributed to the –C=O (–COOH group) and –C–O stretching were also presented at 1629–1630 cm^{-1} and 1067 cm^{-1}, respectively. At wavenumber 1225 cm^{-1}, an additional C–O–C stretching (epoxy group) can only be found on GO-50 spectrum but not GO-30. These results therefore indicate that higher oxidation temperature (50°C) may produce GO with increased oxygen functional groups on its planes, which may consequently make the GO more hydrophilic thus easily dispersed in water.

To further evaluate the effect of oxidation temperatures, Raman spectroscopy was done. As illustrated in Figure 1c, Raman spectrum of graphite powder shows a prominent G band at 1581 cm^{-1}, which corresponds to the first-order Raman band of all sp^2 hybridized carbon materials, and a small D band at 1349 cm^{-1}, which is associated with the defects presence in graphite material.[37,38] In the Raman spectrum of GOs, the G band is broadened and shifted to 1577 cm^{-1} due to the oxidation on the graphite planes. As determined by Lorentzian fitting, the values of intensity ratio of D and G bands (I_D/I_G) ratios of graphite and GOs were 0.201 and 0.986–0.991, respectively. The increase in I_D/I_G ratios following oxidation indicates that GOs have more imperfect structures than graphite due to the generation of epoxide, hydroxyl, and carboxyl groups on their planes.[38] I_D/I_G ratios of GO prepared in this study were higher than that of nano GO synthesized at a higher temperature of 95°C.[25] The I_D/I_G ratio reported in literatures vary widely depending not only on the nature/source of precursor material but also on GO synthesis parameters such as presence of catalyst, amount of reagents, reaction temperature, and residence time. Rao et al. prepared ultrasmall GO nanosheet by using modified method of Marcano and reported an I_D/I_G ratio of 1.03.[20] GO with I_D/I_G ratio of 1.52 could also be attained through a modified Hummers method involving the use of sodium nitrate as catalyst and reaction temperature of 98°C.[38] GO with I_D/I_G ratio as high as 1.2565 could be obtain commercially.[11] The extent of oxidation of graphite to GO thus can be easily tailored as needed by altering the parameters.

There are two weight loss steps observed on TGA thermogram of GO prepared at different reaction temperatures (Figure 1d). The first weight loss at around 100°C is attributed to water evaporation. The second loss at around 200°C corresponds to the decomposition of oxygen functional groups on GO. Since GO-50 has more functional groups on its surface, its thermogram therefore shows higher second decomposition temperature.

Successful preparation of GO was also confirmed by FESEM-EDX analysis, as shown in Figure 2. A flake-like image was observed for graphite material (Figure 2a), compared to a clear GO sheets with slight wrinkles and folds on its surface showing the exfoliated GO layers (Figure 2d). Similar observation was reported by Rattana et al.[39] for their two-dimensional GO nanosheets prepared by a modified Hummers' method. No significant difference was observed between the SEM photos of GO-30 and GO-50. However, the EDX results (Figure S1 and Table S1) revealed that C/O ratios of GO-30 and GO-50 were 2.40 and 1.94, respectively. This result confirms an increase in the amount of oxygen (28.23% for GO-30 to 33.08% for GO-50) following the oxidation of graphite at higher temperatures. A wide range of values

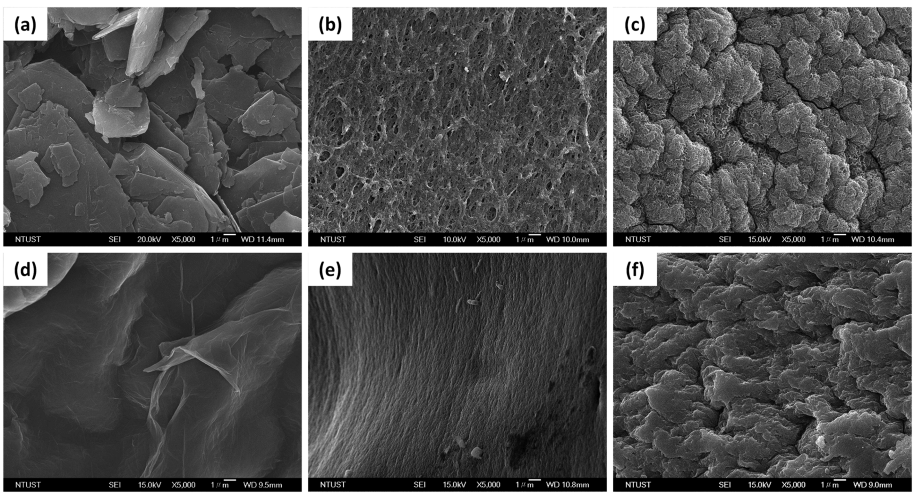

FIGURE 2 FESEM images of (a) graphite, (b) CMC beads, (c) GO/CMC beads, (d) GO, (e) CMC/DOX-loaded beads, and (f) GO/CMC/DOX-loaded beads (scale bar: 1 μm)

was reported in literatures investigating parameters and the extent of oxidation of graphite to GO. The presence of catalyst is commonly expected to improve oxidation efficiency. However, Botas et al.[40] reported lower values of C/O ratios to around 2 with I_D/I_G ratios of 0.89 and 0.92 following oxidation of two synthetic graphites from coal in the presence of catalyst at 98°C. This may be attributed to the difference in source of graphite used as precursor. These results indicate that proper selection of precursor and synthesis parameters are thus crucial to obtain GO with desired functional properties.

3.1 | Preparation and characterizations of GCB

Four types of GCB were prepared in order to study their biocompatibility and capacity as drug carrier. Figure 2 displays FESEM images of pure CMC, GCB, and DOX-loaded GCB. CMC beads showed a uniform and flat but porous surface (Figure 2b), while GCB beads showed a rough surface with slits and wrinkles (Figure 2c). Following drug loading process, the surface of all beads was smoothened to some extent (Figure 2e,f). XRD results presented in Figure S2 clearly show that CMC diffractogram has a small crystalline peak at $2\theta = 19.9°$ which indicates partial crystallinity of CMC.[18,41] In GCB, CMC was successfully introduced between GO layers; therefore, the peak shift of CMC and GO can be observed at $2\theta = 20.8°$ and 13.1°, respectively. These peaks disappeared when DOX was loaded into the beads (shown by GCB/DOX diffractogram).

Figure 3 compares FT-IR patterns of GO, DOX, CMC beads, and the prepared GCB. Figure 3c shows that CMC beads has strong absorption bands at 3407 cm^{-1} (νO–H), 2912 cm^{-1} (νC–H), 1595 cm^{-1} (stretching vibration of carboxylate group), 1428 cm^{-1} (–CH_2 scissoring), 1312 cm^{-1} (–OH bending), and 1060 cm^{-1} (>CH–O–CH_2 stretching), similar to that reported by Liu et al.[16] The occurrence of the hydroxyl group stretching at 2930 cm^{-1} and the characteristic C–H stretching of CH_2 from CMC at 2930 cm^{-1} (Figure 3d) confirmed the successful formation of GCB. The loading of DOX into GCB was displayed by the presence of ketone and benzoquinonyl group of DOX at wavenumber 991 cm^{-1} and 1615 cm^{-1}, respectively.

TGA thermograms of DOX, CMC, GCB, and DOX-loaded beads (GCB/DOX) are presented in Figure S3. Thermograms of GO/CMC hydrogel beads were identical to that of CMC, while hydrogel beads with loaded DOX possessed typical thermogram profiles of CMC and DOX. The residual values at 750°C of GOs, CMC, GCB, CMC/DOX, and GCB/DOX were around 41%, 31%, 32%, 33%, and 30%, respectively. DOX was found to have the highest residual amount (48%).

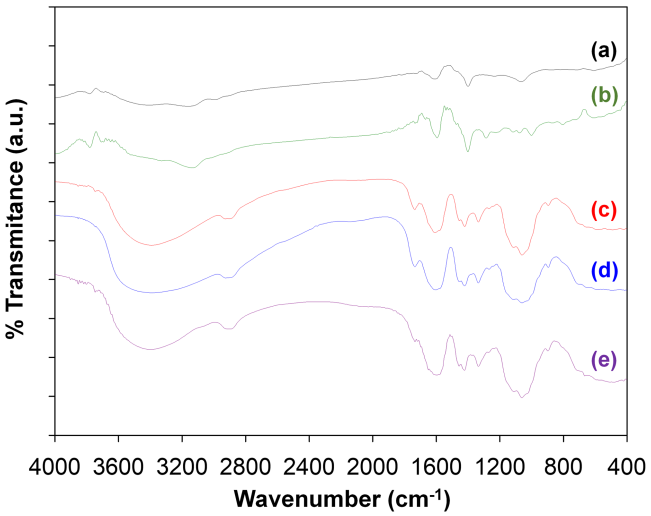

FIGURE 3 FT-IR spectra of (a) GO, (b) DOX, (c) CMC, (d) GCB, and (e) GCB/DOX

3.2 | Swelling behavior of the beads

Swelling properties are essential for hydrogel materials.[16] Prior to drug loading and release studies, the swelling behavior of GO/CMC hydrogel beads was therefore firstly investigated in DI water and PBS solution with various pHs. All hydrogel beads were found to have a low swelling capacity in DI water (20%–30%, data not shown). The swelling capacity of all beads was observed to be higher in PBS solution pH 7.4 than pH 2.1 (Figure 4). This phenomenon was expected since at higher pH; the carboxylic group on GCB was readily deprotonated to form negatively charged carboxyl chains which consequently produce higher electrostatic repulsion within the hydrogel beads; thus, more swelling can be observed. In addition, it can be observed that the swelling capacity of GCBs was increasing with higher amount of GO embedded in beads (GCB-50.5 > GCB-50.1 > GCB 30.5 > GCB-30.1). This trend can be found at any given pH might be influenced by the presence of more oxygen functional group on the GO-rich GCBs.

3.3 | Potential application as drug carrier

The capabilities of GCBs as DOX carrier was investigated, and the results were expressed as DLC. As shown in Figure 5, DLC of DOX into hydrogel beads depended on GO concentration. The DLC of hydrogel beads increased

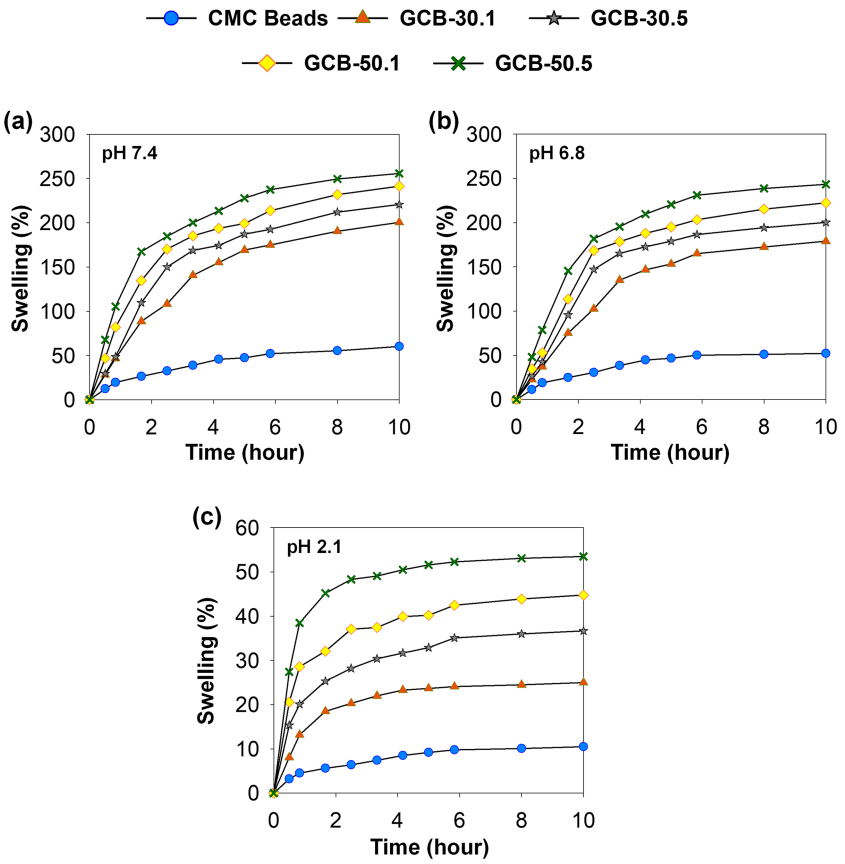

FIGURE 4 Swelling ratio of hydrogel beads in PBS solution with various pH. (GCB-30.1 and GCB-50.1: beads prepared from 1-mg/ml dispersion of GO-30 and GO-50, respectively; GCB-30.5 and GCB-50.5: beads prepared from 5-mg/ml dispersion of GO-30 and GO-50, respectively)

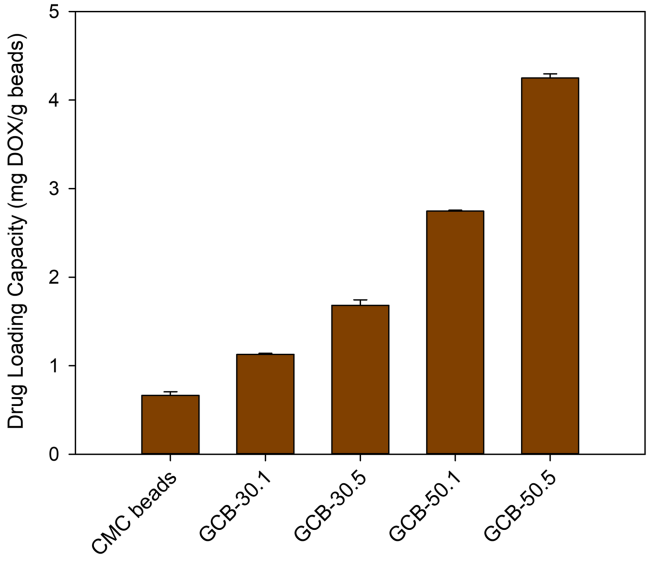

FIGURE 5 Doxorubicin loading on CMC and the as-prepared GO/CMC hydrogel beads (data were presented as mean ± SD [$n = 3$])

with increasing GO concentration, from 0.6647 mg/g for CMC beads to 4.2494 mg/g for GCB-50.5. The trend is in agreement to a study by Javanbakht and Namazi[19] which postulated that the π–π stacking interaction between DOX and oxygen functional groups of GO may account loading mechanism of DOX into GCB. Thus, it is expected that hydrogel beads containing GO prepared at higher oxidation temperature have higher DOX DLC, which is proportional to their oxygen amount (Table S1).

Figure 6 shows DOX cumulative release versus time for hydrogel beads with different GO contents in PBS solutions (pH 5.0 and 7.4). Cumulative DOX release from hydrogel beads decreased significantly with increasing oxidation temperature and GO content. Since higher oxidation temperature resulted in more oxygen functional groups on GO planes, it leads to stronger interactions between amine groups of DOX and carboxylic groups of GO. Higher DOX-release from GO/CMC hydrogel beads can be observed at pH 5.0 system compared to the one at pH 7.4 which is due to their stronger π–π and hydrogen bonding interaction under basic condition than that under acidic condition.

MTT assay was employed to study cytotoxicity of the prepared materials. To date, no study on GO/CMC composites was reported using 7F2 cell lines for in vitro cytotoxicity analysis. This result may also be beneficial for cancer-related bone disease applications. As illustrated in Figure 7, graphite was found to be the most toxic material amongst all. Oxidation of graphite into GO has improved its biocompatibility. Furthermore, most of the as-prepared GO/CMC hydrogel beads have almost no

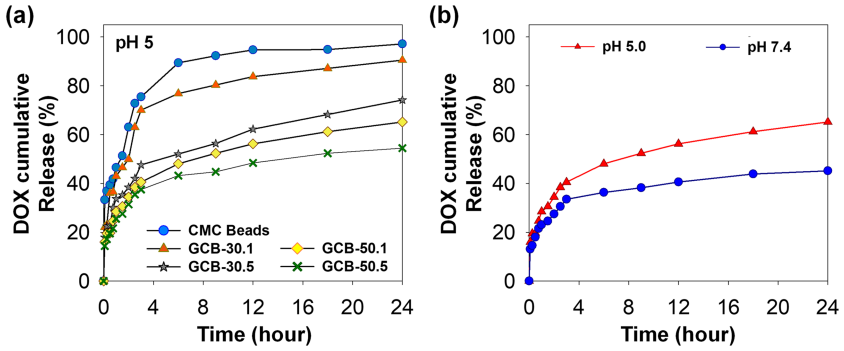

FIGURE 6 Doxorubicin (DOX) release profiles from hydrogel beads in PBS solutions. (a) Percentage of DOX release from CMC beads and GCBs prepared at different oxidation temperatures and varying GO loading in PBS at pH 5. (b) Percentage of DOX release from GCB prepared at 50°C with 5-mg/ml GO loading in PBS

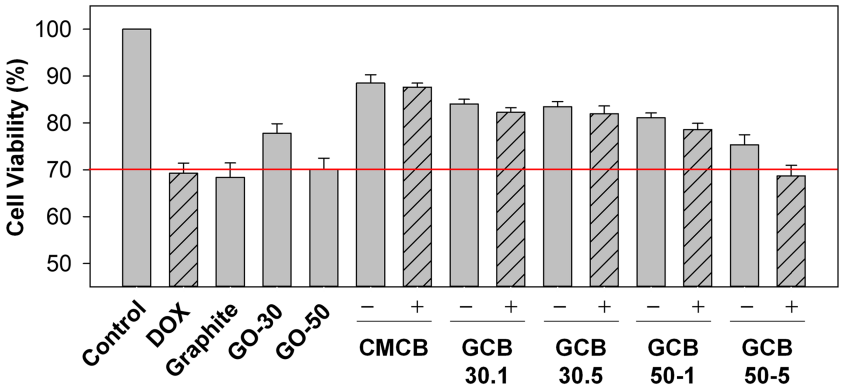

FIGURE 7 In vitro cytotoxicity study of the as-prepared hydrogel beads and its precursor materials. The cell viability of the beads containing DOX (+) and the one without (−) were tested at least three times. Data were presented as mean ± SD

toxic effect on 7F2 cells (above 80% viability). Even though the increase in GO content has raised the toxicity of the beads, but the toxicity level was found to be still within safety range. Additionally, formulation of DOX into hydrogel beads lowered the toxicity of DOX itself (free-DOX). Thus, the newly synthesized GO/CMC composite beads may have potential in improving biocompatibility and provides excellent functional properties, such as pH-responsive drug release.

4 | CONCLUSIONS

In this study, GOs were successfully synthesized using a modest, non-toxic, and eco-friendly approaches of modified Hummers' method. A mild oxidation temperature of 50°C can be chosen to substitute sodium nitrate catalyst in producing GO with satisfactory oxygen functional groups. Results showed that the incorporation of GO into CMC hydrogel beads not only improved the swelling capacity but also proportionally increased the DLC towards DOX. GCB prepared from GO-50 dispersion of 5 mg/ml demonstrated the highest values amongst all due to more oxygen functional groups presented on GO structure. The DLC of GCB increased six-folds compared to that of pure CMC beads. The presence of GO in the hydrogel beads also prolonged the cumulative DOX release into PBS solution at pH 5.0 and 7.4. Due to the incorporation of CMC, the prepared hydrogel beads demonstrated higher cell viability compared to that of their natives GO. The GCB prepared in this study are therefore a promising drug carrier with pH responsive properties.

ACKNOWLEDGEMENT

This study was supported by Ministry of Science and Technology of Taiwan through the project MOST 108-2221-E-011-106 and National Taiwan University of Science and Technology (101H451403).

CONFLICT OF INTEREST

The authors declare no conflict of interest.

ORCID

Artik Elisa Angkawijaya https://orcid.org/0000-0002-4405-5068

REFERENCES

1. Li F, Jiang X, Zhao J, Zhang S. Graphene oxide: a promising nanomaterial for energy and environmental applications. *Nano Energy*. 2015;16:488-515. https://doi.org/10.1016/j.nanoen.2015.07.014
2. Kasturi M, Renu GB, Sivakumar M. Graphene and graphene oxide as a docking station for modern drug delivery system. *Curr Drug Delivery*. 2014;11(6):701-718. https://doi.org/10.2174/1567201811666140605151600

3. Phiri J, Johansson L-S, Gane P, Maloney T. A comparative study of mechanical, thermal and electrical properties of graphene-, graphene oxide- and reduced graphene oxide-doped microfibrillated cellulose nanocomposites. *Compos Part B*. 2018;147:104-113. https://doi.org/10.1016/j.compositesb.2018.04.018
4. Chowdhury S, Balasubramanian R. Recent advances in the use of graphene-family nanoadsorbents for removal of toxic pollutants from wastewater. *Adv Colloid Interf Sci*. 2014;204:35-56. https://doi.org/10.1016/j.cis.2013.12.005
5. Potts JR, Dreyer DR, Bielawski CW, Ruoff RS. Graphene-based polymer nanocomposites. *Polymer*. 2011;52(1):5-25. https://doi.org/10.1016/j.polymer.2010.11.042
6. Bai H, Li C, Wang X, Shi G. A pH-sensitive graphene oxide composite hydrogel. *Chem Commun*. 2010;46(14):2376-2378. https://doi.org/10.1039/C000051E
7. Cong H-P, Wang P, Yu S-H. Stretchable and self-healing graphene oxide–polymer composite hydrogels: a dual-network design. *Chem Mater*. 2013;25(16):3357-3362. https://doi.org/10.1021/cm401919c
8. Yu Y, De Andrade LCX, Fang L, Ma J, Zhang W, Tang Y. Graphene oxide and hyperbranched polymer-toughened hydrogels with improved absorption properties and durability. *J Mater Sci*. 2015;50(9):3457-3466. https://doi.org/10.1007/s10853-015-8905-4
9. Cao L, Zhang F, Wang Q, Wu X. Fabrication of chitosan/graphene oxide polymer nanofiber and its biocompatibility for cartilage tissue engineering. *Mater Sci Eng C*. 2017;79:697-701. https://doi.org/10.1016/j.msec.2017.05.056
10. Deb A, Vimala R. Natural and synthetic polymer for graphene oxide mediated anticancer drug delivery—a comparative study. *Int J Biol Macromol*. 2018;107:2320-2333. https://doi.org/10.1016/j.ijbiomac.2017.10.119
11. Liu Y, Wen J, Gao Y, et al. Antibacterial graphene oxide coatings on polymer substrate. *Appl Surf Sci*. 2018;436:624-630. https://doi.org/10.1016/j.apsusc.2017.12.006
12. Kuila T, Mishra AK, Khanra P, Kim NH, Lee JH. Recent advances in the efficient reduction of graphene oxide and its application as energy storage electrode materials. *Nanoscale*. 2013;5(1):52-71. https://doi.org/10.1039/C2NR32703A
13. Guo H, Li T, Cao X, et al. Self-fterilized flexible single-electrode triboelectric nanogenerator for energy harvesting and dynamic force sensing. *ACS Nano*. 2017;11(1):856-864. https://doi.org/10.1021/acsnano.6b07389
14. Gultom NS, Abdullah H, Kuo D-H, Simamora P, Sirait M. Development photocatalyst reduce graphene oxide (RGO) composited with (Zn,Ni)(O,S) for photocatalytic hydrogen production. *J Phys Conf Ser*. 2019;1230:1-6. https://doi.org/10.1088/1742-6596/1230/1/012102
15. Ahmed F, Rodrigues DF. Investigation of acute effects of graphene oxide on wastewater microbial community: a case study. *J Hazard Mater*. 2013;256–257:33-39. https://doi.org/10.1016/j.jhazmat.2013.03.064
16. Liu J, Chu H, Wei H, et al. Facile fabrication of carboxymethyl cellulose sodium/graphene oxide hydrogel microparticles for water purification. *RSC Adv*. 2016;6(55):50061-50069. https://doi.org/10.1039/C6RA06438H
17. Abd-Elhamid AI, Aly HF, Soliman HAM, El-Shanshory AA. Graphene oxide: follow the oxidation mechanism and its application in water treatment. *J Mol Liq*. 2018;265:226-237. https://doi.org/10.1016/j.molliq.2018.05.127
18. Rasoulzadeh M, Namazi H. Carboxymethyl cellulose/graphene oxide bio-nanocomposite hydrogel beads as anticancer drug carrier agent. *Carbohydr Polym*. 2017;168:320-326. https://doi.org/10.1016/j.carbpol.2017.03.014
19. Javanbakht S, Namazi H. Doxorubicin loaded carboxymethyl cellulose/graphene quantum dot nanocomposite hydrogel films as a potential anticancer drug delivery system. *Mater Sci Eng C*. 2018;87:50-59. https://doi.org/10.1016/j.msec.2018.02.010
20. Rao Z, Ge H, Liu L, et al. Carboxymethyl cellulose modified graphene oxide as pH-sensitive drug delivery system. *Int J Biol Macromol*. 2018;107:1184-1192. https://doi.org/10.1016/j.ijbiomac.2017.09.096
21. Yang H, Bremner DH, Tao L, Li H, Hu J, Zhu L. Carboxymethyl chitosan-mediated synthesis of hyaluronic acid-targeted graphene oxide for cancer drug delivery. *Carbohydr Polym*. 2016;135:72-78. https://doi.org/10.1016/j.carbpol.2015.08.058
22. Tran TH, Nguyen HT, Pham TT, et al. Development of a graphene oxide nanocarrier for dual-drug chemo-phototherapy to overcome drug resistance in cancer. *ACS Appl Mater Interfaces*. 2015;7(51):28647-28655. https://doi.org/10.1021/acsami.5b10426
23. Zhou T, Zhou X, Xing D. Controlled release of doxorubicin from graphene oxide based charge-reversal nanocarrier. *Biomaterials*. 2014;35(13):4185-4194. https://doi.org/10.1016/j.biomaterials.2014.01.044
24. Yang X, Zhang X, Liu Z, Ma Y, Huang Y, Chen Y. High-efficiency loading and controlled release of doxorubicin hydrochloride on graphene oxide. *J Phys Chem C*. 2008;112(45):17554-17558. https://doi.org/10.1021/jp806751k
25. Wang L, Yu D, Dai R, et al. PEGylated doxorubicin cloaked nano-graphene oxide for dual-responsive photochemical therapy. *Int J Pharm*. 2019;557:66-73. https://doi.org/10.1016/j.ijpharm.2018.12.037
26. Kazempour M, Namazi H, Akbarzadeh A, Kabiri R. Synthesis and characterization of PEG-functionalized graphene oxide as an effective pH-sensitive drug carrier. *Artificial Cells, Nanomedicine, and Biotechnology*. 2019;47(1):90-94. https://doi.org/10.1080/21691401.2018.1543196
27. Mejías Carpio IE, Santos CM, Wei X, Rodrigues DF. Toxicity of a polymer–graphene oxide composite against bacterial planktonic cells, biofilms, and mammalian cells. *Nanoscale*. 2012;4(15):4746-4756. https://doi.org/10.1039/C2NR30774J
28. Dimiev A, Kosynkin DV, Alemany LB, Chaguine P, Tour JM. Pristine graphite oxide. *J Am Chem Soc*. 2012;134(5):2815-2822. https://doi.org/10.1021/ja211531y
29. Yadav M, Rhee KY, Park SJ. Synthesis and characterization of graphene oxide/carboxymethylcellulose/alginate composite blend films. *Carbohydr Polym*. 2014;110:18-25. https://doi.org/10.1016/j.carbpol.2014.03.037
30. Li Y, Jiang L. Preparation of graphene oxide–chitosan nanocapsules and their applications as carriers for drug delivery. *RSC Adv*. 2016;6(106):104522-104528. https://doi.org/10.1039/C6RA24401G
31. Zhang Y, Zhang M, Jiang H, et al. Bio-inspired layered chitosan/graphene oxide nanocomposite hydrogels with high strength and pH-driven shape memory effect. *Carbohydr*

Polym. 2017;177:116-125. https://doi.org/10.1016/j.carbpol.2017.08.106

32. Piao Y, Chen B. Self-assembled graphene oxide–gelatin nanocomposite hydrogels: characterization, formation mechanisms, and pH-sensitive drug release behavior. *J Polym Sci B Polym Phys*. 2015;53(5):356-367. https://doi.org/10.1002/polb.23636
33. Singh AK, Basavaraju KC, Sharma S, Jang S, Park CP, Kim D-P. Eco-efficient preparation of a N-doped graphene equivalent and its application to metal free selective oxidation reaction. *Green Chem*. 2014;16(6):3024-3030. https://doi.org/10.1039/C4GC00049H
34. Wang MO, Etheridge JM, Thompson JA, Vorwald CE, Dean D, Fisher JP. Evaluation of the in vitro cytotoxicity of cross-linked biomaterials. *Biomacromolecules*. 2013;14(5):1321-1329. https://doi.org/10.1021/bm301962f
35. Hontoria-Lucas C, López-Peinado AJ, López-González J d D, Rojas-Cervantes ML, Martín-Aranda RM. Study of oxygen-containing groups in a series of graphite oxides: physical and chemical characterization. *Carbon*. 1995;33(11):1585-1592. https://doi.org/10.1016/0008-6223(95)00120-3
36. Marcano DC, Kosynkin DV, Berlin JM, et al. Improved synthesis of graphene oxide. *ACS Nano*. 2010;4(8):4806-4814. https://doi.org/10.1021/nn1006368
37. Ferrari AC. Raman spectroscopy of graphene and graphite: disorder, electron–phonon coupling, doping and nonadiabatic effects. *Solid State Commun*. 2007;143(1):47-57. https://doi.org/10.1016/j.ssc.2007.03.052
38. Dubale AA, Su W-N, Tamirat AG, et al. The synergetic effect of graphene on Cu2O nanowire arrays as a highly efficient hydrogen evolution photocathode in water splitting. *J Mater Chem A*. 2014;2(43):18383-18397. https://doi.org/10.1039/C4TA03464C
39. Rattana, Chaiyakun S, Witit-anun N, et al. Preparation and characterization of graphene oxide nanosheets. *Procedia Eng*. 2012;32:759-764. https://doi.org/10.1016/j.proeng.2012.02.009
40. Botas C, Álvarez P, Blanco C, et al. The effect of the parent graphite on the structure of graphene oxide. *Carbon*. 2012;50(1):275-282. https://doi.org/10.1016/j.carbon.2011.08.045
41. Dahlan NA, Pushpamalar J, Veeramachineni AK, Muniyandy S. Smart hydrogel of carboxymethyl cellulose grafted carboxymethyl polyvinyl alcohol and properties studied for future material applications. *J Polym Environ*. 2018;26(5):2061-2071. https://doi.org/10.1007/s10924-017-1105-3

SUPPORTING INFORMATION

Additional supporting information may be found online in the Supporting Information section at the end of this article.

How to cite this article: Ayucitra A, Angkawijaya AE, Ju Y-H, Gunarto C, Go AW, Ismadji S. Graphene oxide-carboxymethyl cellulose hydrogel beads for uptake and release study of doxorubicin. *Asia-Pac J Chem Eng*. 2021;16:e2646. https://doi.org/10.1002/apj.2646